Quenching of the SnSbTe Cycle in the *rp* Process

V.-V. Elomaa,[1,*] G. K. Vorobjev,[2,3] A. Kankainen,[1] L. Batist,[2] S. Eliseev,[2,3,†] T. Eronen,[1] J. Hakala,[1] A. Jokinen,[1] I. D. Moore,[1] Yu. N. Novikov,[2,3] H. Penttilä,[1] A. Popov,[2] S. Rahaman,[1,‡] J. Rissanen,[1] A. Saastamoinen,[1] H. Schatz,[4] D. M. Seliverstov,[2] C. Weber,[1,§] and J. Äystö[1]

[1]*Department of Physics, University of Jyväskylä, Post Office Box 35, FI-40014, Finland*
[2]*Petersburg Nuclear Physics Institute, 188300 Gatchina, Russia*
[3]*Gesellschaft für Schwerionenforschung mbH, Planckstraße 1, D-64291 Darmstadt, Germany*
[4]*Department of Physics and Astronomy, National Superconducting Cyclotron Laboratory, and Joint Institute for Nuclear Astrophysics, Michigan State University, East Lansing, Michigan 48824, USA*

(Received 17 February 2009; published 25 June 2009)

The nuclides $^{104-108}$Sn, $^{106-110}$Sb, ^{108,109}Te, and ^{111}I at the expected endpoint of the astrophysical *rp* process have been produced in ^{58}Ni + ^{nat}Ni fusion-evaporation reactions at IGISOL and their mass values were precisely measured with the JYFLTRAP Penning trap mass spectrometer. For ^{106}Sb, ^{108}Sb, and ^{110}Sb these are the first direct experimental mass results obtained. The related one-proton separation energies have been derived and the value for ^{106}Sb, $S_p = 424(8)$ keV, shows that the branching into the closed SnSbTe cycle in the astrophysical *rp* process is weaker than expected.

DOI: 10.1103/PhysRevLett.102.252501 PACS numbers: 21.10.Dr, 26.30.−k, 26.50.+x, 27.60.+j

The astrophysical rapid-proton-capture process (*rp* process) [1], a sequence of rapid proton captures and β^+ decays close to the proton drip line, powers the frequently observed type I x-ray bursts [2] occurring on the surface of mass-accreting neutron stars. The path of the *rp* process determines the shape of the observed x-ray light curve and the composition of the burst ashes. Most of the burst ashes are eventually incorporated into the neutron star crust, and nuclear heating processes that could explain observations of superbursts and cooling transients depend very sensitively on their composition [3]. It is possible that a small fraction of the ashes may be ejected. In order to estimate abundance signatures for future x-ray observation searches, the ash composition must be known [4]. Additionally, the composition determines whether x-ray bursts might contribute to the origin of some of the light *p* nuclei in the $A = 92$–98 mass range, that are found with so far unexplained large abundance in the Solar System [5].

A particularly important issue is that of the existence of an endpoint to the *rp* process for the specific conditions of a given x-ray burst. Network calculations indicate that the *rp* process in x-ray bursts cannot proceed past tellurium and is limited by a SnSbTe cycle [6]. Within the tellurium isotopes a small island of α radioactivity stops the further development of the *rp* process towards heavier nuclides.

The SnSbTe cycle not only limits the production of heavier elements, therefore strongly affecting the composition of the burst ashes, but also leads to additional helium production towards the end of the burst that can boost energy generation and hydrogen consumption via a more efficient 3α process, providing additional seeds for the *rp* process. In principle, this could affect the tail of the burst light curve [6].

However, whether the SnSbTe cycle is reached and to which degree it can operate, depends strongly on the nuclear masses and, in particular, on the proton separation energies of the neutron-deficient antimony isotopes. Numerous precise Penning trap mass determinations for nuclides along the *rp*-process path around $A = 80$–100 have been performed at JYFLTRAP [7–9]. In addition, masses for nuclides with $A = 99$–113, such as ^{105,106}Sn and ^{107}Sb, have been measured at the SHIPTRAP Penning trap mass spectrometer at GSI/Darmstadt [10]. Separately, the α-decay energy of ^{109}I has been determined at the HRIBF, Oak Ridge National Laboratory [11]. In this Letter, we report on the latest results from JYFLTRAP that have reached sufficiently neutron-deficient rare isotopes to allow one to address the questions of the existence and the strength of a SnSbTe cycle in x-ray bursts.

The nuclides of interest were produced by a 295–330 MeV ^{58}Ni beam impinging on a rotating ^{nat}Ni target of thickness 4 mg/cm^2. The reaction products were stopped in the HIGISOL [12] gas cell, extracted, accelerated, and mass separated prior to their transfer to JYFLTRAP. After mass separation, the ions were injected into a gas-filled radiofrequency quadrupole (RFQ) [13] for cooling and bunching. The cooled ion bunches were transported into the JYFLTRAP system consisting of two cylindrical Penning traps inside a superconducting magnet with a field strength of $B = 7$ T. The first trap, with a mass resolving power of about 10^5, is used for isobaric purification. The precision mass measurements are performed in the second trap. The cyclotron frequency $\nu_c = qB/(2\pi m)$ is determined via the time-of-flight ion cyclotron resonance method [14] for an ion with charge $q = 1+$ and mass m. As an example, two cyclotron resonance curves for the shortest-lived nuclides in our *rp*-process study are shown in Fig. 1.

To determine the mass from the cyclotron frequency, the magnitude of the magnetic field has to be known very

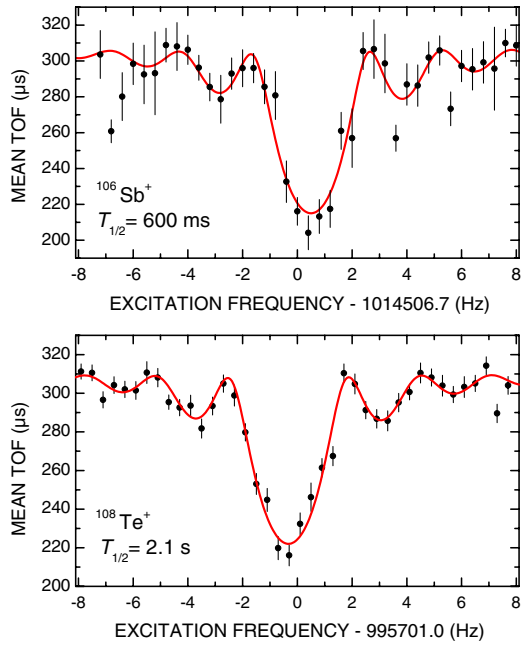

FIG. 1 (color online). Time-of-flight (TOF) cyclotron resonance curves for the shortest-lived nuclides measured in this work, ^{106}Sb and ^{108}Te.

accurately. This is achieved by a determination of the cyclotron frequencies $\nu_{c,\mathrm{ref}}$ of an ion with a well-known mass value, before and after the measurement of the ion of interest. In this experiment, $^{87}Rb^{+}$ ions with a mass uncertainty of $\delta m = 12$ eV [15] have been used. The atomic mass m of the nuclide of interest is obtained from the frequency ratio $r = \frac{\nu_{c,\mathrm{ref}}}{\nu_c}$ of the reference ion and the ion of interest. The analysis of the data was performed according to the description given in Ref. [8], whereas a value of $\sigma_B(\nu_{\mathrm{ref}})/\nu_{\mathrm{ref}} = [5.7(8) \times 10^{-11}\ \mathrm{min}^{-1}]\Delta t$ was used as the relative uncertainty in the time variation of the magnetic field strength. The masses of $^{104-108}$Sn, $^{106-110}$Sb, ^{108,109}Te, and ^{111}I have been more precisely determined, whereas the values for ^{106}Sb, ^{108}Sb, and ^{110}Sb are the first experimental determinations. All results obtained in this work are listed in Table I.

The one-proton separation energies S_p for nuclides of interest for the SnSbTe cycle are given in Table II and are shown in Fig. 2. They were determined using directly measured masses and those derived via combinations with α or p decay Q values. Isotopes of cadmium and indium have been recently studied at JYFLTRAP [9] and the masses of several isotopes from cadmium to xenon were determined at SHIPTRAP [10]. Since these data are also relevant for the endpoint region of the rp process, a weighted average of all Penning trap results was used in the calculation of proton separation energies. For cadmium and indium, data have been averaged from Refs. [9,10] ($^{101-104}$Cd, ^{102,104}In), for ^{105,106}Sn, ^{107,109}Sb, ^{109}Te, and ^{111}I weighted means of the results from this work and Ref. [10] have been used. The masses of ^{103,105}In, ^{110,111}Te, ^{112}I, and ^{113}Xe have been taken from Ref. [10]. The masses for ^{104,107,108}Sn, ^{106,108,110}Sb, and ^{108}Te are exclusively from this work. For further nuclides, the values from AME2003 [15] were used.

TABLE I. Frequency ratios r, mass excess values (ME), and literature values ($\mathrm{ME_{lit}}$) from SHIPTRAP [10] or AME2003 [15]. The superscript # indicates a value that has been extrapolated from systematic trends. The atomic mass of ^{87}Rb [15] was used as a reference.

Nuclide	$r = \frac{\nu_{c,\mathrm{ref}}}{\nu_c}$	ME (keV)	$\mathrm{ME_{lit}}$(keV)
^{104}Sn	1.195 767 977(74)	−71 625(6)	−71 590(100) [15]
^{105}Sn	1.207 253 180(64)	−73 336(5)	−73 342(7) [10]
^{106}Sn	1.218 709 913(87)	−77 351(7)	−77 350(8) [10]
^{107}Sn	1.230 201 911(65)	−78 512(5)	−78 580(80) [15]
^{108}Sn	1.241 664 284(68)	−82 071(6)	−82 041(20) [15]
^{106}Sb	1.218 844 285(92)	−66 473(7)	−66 330(310)# [15]
^{107}Sb	1.230 299 077(67)	−70 646(5)	−70 663(10) [10]
^{108}Sb	1.241 783 189(68)	−72 445(6)	−72 510(210)# [15]
^{109}Sb	1.253 242 516(68)	−76 251(5)	−76 279(17) [10]
^{110}Sb	1.264 734 046(73)	−77 450(6)	−77 540(200)# [15]
^{108}Te	1.241 865 478(69)	−65 784(6)	−65 720(100) [15]
^{109}Te	1.253 347 956(73)	−67 715(6)	−67 714(8) [10]
^{111}I	1.276 394 688(70)	−64 958(6)	−64 973(18) [10]

For nuclear astrophysics, the most interesting nuclei in this mass region are the antimony isotopes. Being only slightly proton-bound or even proton-unbound, they act as a gate for the rp-process flow towards the region of α radioactivity at the tellurium isotopes. Recently, a negative proton separation energy for ^{105}Sb [$S_p = -356(22)$ keV] has been indirectly determined from the measurement of the α-decay energy of ^{109}I [11] and by using S_p for ^{109}I and Q_α for ^{108}Te [15].

It should be noted that the Q_α values for ^{108}Te and ^{109}Te calculated from our measured mass differences are about 30(9) keV smaller than the values extracted from the measured α-decay energies; see Ref. [16]. Though our

TABLE II. Proton separation energies S_p determined in this work.

Nuclide	S_p(keV)	Nuclide	S_p(keV)
^{104}Sn	4277(12)	^{106}Te	1520(130)[a]
^{105}Sn	4448(6)	^{107}Te	1360(300)[b]
^{106}Sn	4999(11)	^{108}Te	2424(7)
^{107}Sn	5195(13)	^{109}Te	2559(8)
^{108}Sn	5800(13)	^{110}Te	3271(8)
^{106}Sb	424(8)	^{111}Te	3426(8)
^{107}Sb	588(7)	^{110}I	42(51)[c]
^{108}Sb	1222(8)	^{111}I	13(9)
^{109}Sb	1471(8)	^{112}Xe	2359(10)[c]
^{110}Sb	2100(12)	^{114}Cs	−230(59)[c]

[a] S_p derived employing the mass of ^{106}Te [15], ^{104}Sn [this work] and $Q_p(^{105}\mathrm{Sb})$ [11].
[b] S_p derived employing the extrapolated mass of ^{107}Te from [15].
[c] Mass derived using Q_α of the respective nuclide [15].

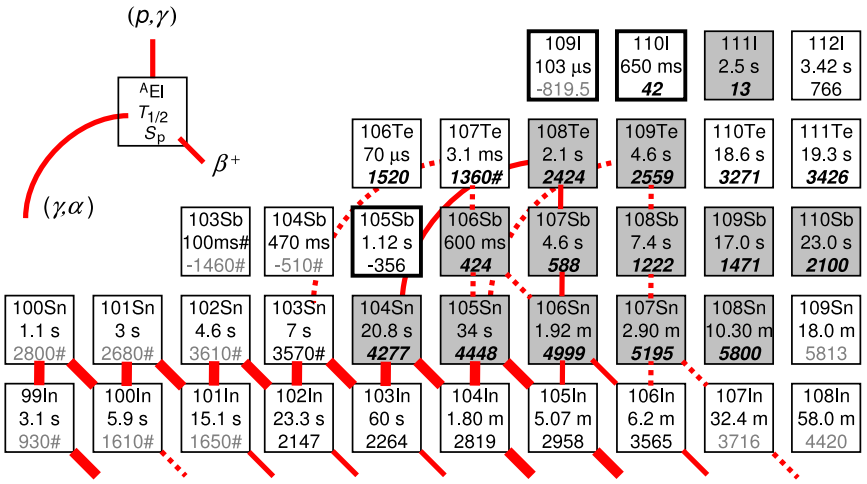

FIG. 2 (color online). Nuclear chart in the region of the expected rp-process endpoint. Nuclides studied in this work are shown in gray. For nuclides enclosed with a bold box, the values were derived via proton or α decay Q values. Several values are improved by the data obtained in this work (bold face, italic). The other S_p values are taken from recent experiments [9–11] (normal font), or the AME2003 [15] (gray font). Thick solid lines, thin solid lines, and dotted lines represent time-integrated reaction flows over the entire burst calculations with magnitudes of more than 10%, more than 1% and more than 0.1% of the flow through the 3α reaction, respectively.

measurements revise these Q_α values that had been used to calibrate the experiment of Ref. [11], the resulting $S_p(^{105}\mathrm{Sb})$ is unaffected by this change because it is based on the difference of two Q_α values. The proton separation energy for ^{104}Sb was estimated to be $S_p > -378$ keV in Ref. [11] suggesting that ^{104}Sb might be proton-unbound as well. As it was shown, these S_p values prevent the development of the rp process via ^{104}Sb and ^{105}Sb towards the α-decay region, e.g., to recycling. Because of the proton-unbound nuclides ^{104}Sb and ^{105}Sb, the rp process has to proceed along the tin isotopes to ^{105}Sn. After ^{105}Sn, the path depends on the strength of the proton binding of ^{106}Sb. Only one measurement for ^{106}Sb had been performed earlier [17]. The result, $S_p = 930(210)$ keV, gives the rp flow branching into a SnSbTe cycle on the level of 50(30)% (according to Fig. 4 in Ref. [11]). The new value, $S_p = 424(8)$ keV, obtained in this work (see Table II), disagrees considerably with the one of Ref. [17], which was not adopted in the Atomic Mass Evaluation which instead gives an extrapolated value of $S_p(^{106}\mathrm{Sb}) = 360(320)^{\#}$ keV [15].

We used the same one-zone model as in Ref. [11] to explore the consequences of the new ^{106}Sb proton separation energy on x-ray bursts. The parameters of this model have been chosen to study model conditions that are most favorable for reaching the SnSbTe region. The reaction flow reaches ^{105}Sn towards the end of the burst with a maximum of the abundance reached about 160 s after the burst peak. We find that with our new masses only 3% of the reaction flow branches into the SnSbTe cycle at ^{105}Sn, thus considerably attenuating the cycling via the chain ^{105}Sn-^{106}Sb-^{107}Te-^{103}Sn-^{103}In-^{104}Sn-^{104}In-^{105}Sn.

The next possibility for forming a cycle is at ^{106}Sn by proton capture through ^{107}Sb, but with a proton separation energy of only 588(7) keV we find only a 13% branch. ^{108}Sb has a much larger proton separation energy, but at this point the delay imposed by the long β-decay half-life of ^{106}Sn of 2 min inhibits further processing before the burst ends. Nevertheless, the burst still burns all its initial hydrogen as there is enough intermediate mass ashes present that is still being processed by rapid-proton capture.

Previous calculations had assumed there is a strong SnSbTe cycle through ^{106}Sb leading to a large accumulation of ^{104}Sn, which is the longest-lived isotope in the SnSbTe cycle in this case. This is depicted in Fig. 3 where

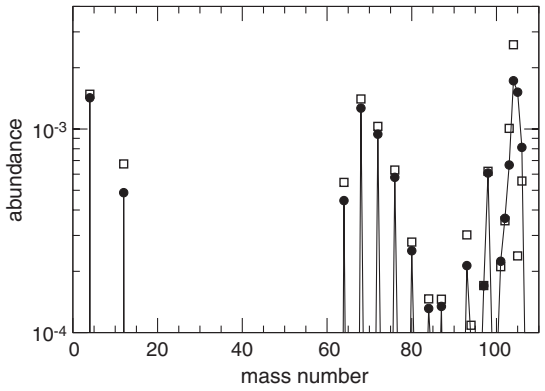

FIG. 3. Final composition of the burst ashes for a ^{106}Sb proton separation energy of 1350 keV (2σ upper value from previous work, white squares) and 424 keV (this work, black circles). Shown is the summed abundance (mass fraction divided by mass number) of an isobaric mass chain as a function of mass number. After a sufficiently long time, the neutron-deficient isotopes will have decayed into the first stable isotope encountered in each mass chain. The residual helium will eventually be burned into ^{12}C and possibly some heavier α-capture isotopes.

we show the final composition of the ashes as a function of mass number for a calculation based on the 2σ upper limit of the previous ^{106}Sb proton separation energy (1350 keV) that leads to a very strong SnSbTe cycle. ^{104}Pd is by far the most abundant element in the final ashes and therefore the underlying liquid ocean covering the surface of the neutron star, with a total mass fraction of almost 30%. On the other hand, with our new masses such a strong cycle scenario can now be excluded with high confidence. Cycling is now almost absent, and the final composition is characterized by a broader distribution of ^{68}Zn, ^{72}Ge, ^{104}Pd, ^{105}Pd, and residual helium with comparable abundances. This will change the heating pattern in the crust [3] and the larger degree of impurity will lead to changes in the thermal conductivity of the crust.

The absence of a strong SnSbTe cycle also reduces late-time ^{4}He production, the main product of the SnSbTe cycle. This reduces the late-time boost of hydrogen consumption (as new seed nuclei are produced) and the associated boost in energy production caused by the SnSbTe cycle, leading to a slightly longer, less luminous burst tail [6]. However, this effect is small, as even in the strong cycling case the SnSbTe cycle at ^{105}Sn is only reached at a very late stage in the burst in the present model. Less cycling also leads to a reduction of residual ^{4}He and ^{12}C. Assuming that all residual ^{4}He will eventually be processed into ^{12}C, the final ^{12}C mass fraction is reduced from 1.4% to 1.2%. Again, this is a small effect but makes it even harder to explain the origin of large amounts of residual ^{12}C of the order of 10% required by current superburst models [18].

With the present measurements, the masses needed to constrain the reaction flows in the endpoint region of the rp process are now determined. The main remaining uncertainties are the proton-capture rates on the antimony isotopes, in particular ^{105}Sb and ^{106}Sb. As (p, γ)-(γ, p) equilibrium is likely to be established between the antimony and tin isotopes, an increase in these reaction rates could increase the amount of cycling in the SnSbTe cycles [11]. Rapp *et al.* [19] estimate proton-capture reaction rate uncertainties to vary up to a factor of 3 close to stability, whereas uncertainties far from stability might be larger. The ^{106}Sb(p, γ) rate of Ref. [20] is about a factor of 4 larger than the NON-SMOKER [21] rate used here. Therefore, branchings into the SnSbTe cycle of the order of 10% at ^{105}Sn might be possible, still significantly below the 50% branching assumed previously. While direct measurements of the ^{106}Sb(p, γ) reaction rate with radioactive beams remain likely out of reach for the time being, indirect studies of the level structure in ^{107}Te above the proton threshold might help constrain this rate and therefore the strength of the SnSbTe cycle in x-ray bursts.

In summary, mass values for 13 nuclides in or near the expected endpoint region of the rp process have been directly measured with the JYFLTRAP Penning trap. Contrary to previous calculations, the new experimental value of $S_p = 424(8)$ keV for ^{106}Sb excludes the possibility of a strong SnSbTe cycle starting at ^{105}Sn. Hence, the rp-process path moves closer to stability before a SnSbTe cycle forms. This will affect the composition of the ashes of type I x-ray bursts and avoids the consequences a strong SnSbTe cycle would have on the burst light curve.

This work has been supported by the EU 6th Framework programme ''Integrating Infrastructure Initiative—Transnational Access'', Contract No.: 506065 (EURONS) and by the Academy of Finland under the Finnish Center of Excellence Programme 2006–2011 (Nuclear and Accelerator Based Physics Programme at JYFL). The support via the Finnish-Russian Interacademy Agreement (Project No. 8) is acknowledged. H. S. is supported by NSF Grants PHY-0606007 and PHY-0822648.

*viki-veikko.v.elomaa@jyu.fi

†Present address: Max-Planck-Institut für Kernphysik, D-69117 Heidelberg, Germany.

‡Present address: Physics Division, P-23, Mail Stop H803, Los Alamos National Laboratory, Los Alamos, NM 87545, USA.

§Present address: Fakultät für Physik, Ludwig-Maximilians-Universität München, Am Coulombwall 1, D-85748 Garching, Germany.

[1] R. Wallace and S. Woosley, Astrophys. J. Suppl. Ser.. **45**, 389 (1981).
[2] H. Schatz and K. E. Rehm, Nucl. Phys. **A777**, 601 (2006).
[3] S. Gupta *et al.*, Astrophys. J. **662**, 1188 (2007).
[4] N. N. Weinberg, L. Bildsten, and H. Schatz, Astrophys. J. **639**, 1018 (2006).
[5] M. Arnould and S. Goriely, Phys. Rep. **384**, 1 (2003).
[6] H. Schatz *et al.*, Phys. Rev. Lett. **86**, 3471 (2001).
[7] A. Kankainen *et al.*, Eur. Phys. J. A **29**, 271 (2006).
[8] C. Weber *et al.*, Phys. Rev. C **78**, 054310 (2008).
[9] V.-V. Elomaa *et al.*, Eur. Phys. J. A **40**, 1 (2009).
[10] A. Martín *et al.*, Eur. Phys. J. A **34**, 341 (2007).
[11] C. Mazzocchi *et al.*, Phys. Rev. Lett. **98**, 212501 (2007).
[12] J. Äystö, Nucl. Phys. **A693**, 477 (2001).
[13] A. Nieminen *et al.*, Nucl. Instrum. Methods Phys. Res., Sect. A **469**, 244 (2001).
[14] M. König *et al.*, Int. J. Mass Spectrom. Ion Processes **142**, 95 (1995).
[15] G. Audi, A. H. Wapstra, and C. Thibault, Nucl. Phys. A **729**, 337 (2003).
[16] F. Heine *et al.*, Z. Phys. A **340**, 225 (1991).
[17] A. Plochocki *et al.*, Phys. Lett. B **106**, 285 (1981).
[18] A. Cumming, J. Macbeth, J. J. M. in 't Zand, and D. Page, Astrophys. J. **646**, 429 (2006).
[19] W. Rapp *et al.*, Astrophys. J. **653**, 474 (2006).
[20] M. Aikawa *et al.*, Astron. Astrophys. **441**, 1195 (2005).
[21] T. Rauscher *et al.*, At. Data Nucl. Data Tables **79**, 47 (2001).